Nanoscale

RSC Publishing

PAPER

View Article Online
View Journal | View Issue

Cite this: *Nanoscale*, 2013, **5**, 8577

Cellular interactions of doxorubicin-loaded DNA-modified halloysite nanotubes†

Yeonju Lee,[a] Goo-Eun Jung,[b] Sang Joon Cho,[bc] Kurt E. Geckeler*[def] and Harald Fuchs*[aeg]

Received 22nd May 2013
Accepted 2nd July 2013

DOI: 10.1039/c3nr02665e

www.rsc.org/nanoscale

Halloysite nanotube (HNT)-based supramolecular complexes are synthesized and evaluated with respect to their cytotoxicity and effects on cellular structures. As HNTs are water-insoluble, DNA is applied for wrapping the surface of HNTs to enhance their water-dispersibility. To investigate the potential of DNA-wrapped HNTs (HD) as a promising drug delivery carrier, doxorubicin (DOX) is introduced as a model anticancer agent and loaded onto HD. The DOX-loaded, DNA-wrapped HNTs (HDD) show sustained DOX release over two weeks without initial burst of DOX indicating delayed DOX release inside cells. In addition, effects of DNA-wrapped HNTs (HD) or HDD on the cytoskeleton organization of A549 cells are studied by visualizing the distribution of F-actin filaments using confocal laser scanning microscopy, and cellular morphological changes are observed by scanning electron microscopy and scanning ion conductance microscopy.

Introduction

Due to interesting physico-chemical characteristics and biocompatibility of halloysite ($Al_2Si_2O_5(OH)_4 \cdot 2H_2O$) nanotubes (HNTs), they have recently attracted great interest for application in nanotechnology and biotechnology.[1,2] Halloysite is chemically similar to kaolin, which is a dioctahedral 1 : 1 layered clay mineral of structural formula $Al_2Si_2O_5(OH)_4$.[3] Its morphology mainly differs from kaolin, which exhibits a stacked plate-like structure. HNTs have a hollow tubular structure with a size varying from 500–1000 nm in length and 15–100 nm in diameter.[1,2,4] Their hollow nanotubular structure provides space for encapsulating a range of active agents.[5] Specifically, different surface chemistry of the inner and outer surfaces of HNTs, *i.e.* a negatively charged outer surface and a positively charged inner lumen surface in the pH range 2–8, allows selective modifications.[6] It is possible to load anionic agents by entrapment into its hollow lumen or cationic agents on the nanotube surface.[7]

HNTs occur in nature and they are not hazardous and expensive compared to other types of nanotubes, for example, carbon nanotubes.[2,5,8–10] HNT-coated substrates[11] or HNT/polymer bio-active nanocomposite films[12] are used for cell culture substrates. Attachment and spreading of human dermal fibroblast cells were shown to be faster on HNT-coated substrates than on silica or montmorillonite coated films.[11] The osteoblast and fibroblast cells adhere well on nano-biocomposite films containing a biodegradable polymer, such as poly(vinyl alcohol) (PVA) and HNTs.[12] In addition, chitosan/HNT nanocomposites show promising properties as 3T3 cell culture substrates.[13] Recently, cytotoxicity of pristine HNTs or functionalized HNTs on mammalian cells such as 3T3,[14] MCF7,[5,14] and HeLa cells[5] was reported. Based on the biocompatibility of HNTs, they are applied for drug[15–19] or gene delivery systems.[20] For instance, tetracycline hydrochloride loaded HNTs mixed with poly(lactic-*co*-glycolic acid) (PLGA) form drug-loaded composite nanofibrous mats *via* electrospinning. They show a prolonged release duration of the drug.[19] Also, the hybrid materials based on HNTs, poly(vinyl alcohol), and diphenhydramine hydrochloride, are suggested to be an ideal drug delivery system.[18]

In this study, cellular interactions of HNT-based supramolecular complexes are described. Based on our previous study concerning the formation of water-dispersible HNTs by wrapping with a biopolymer, DNA,[4] here, we suggest DNA-wrapped HNTs (HD) as a doxorubicin delivery carrier. Doxorubicin (DOX) is one of the well-established and effective anticancer drugs against various types of cancers.[21] It binds to DNA-associated enzymes, intercalates with DNA base pairs, and then prohibits the tumor cells from further division.[22] Here, cytotoxicity and effects of HD

[a]*Physikalisches Institut, Universität Münster, Wilhelm Klemm-Str. 10, 48149 Münster, Germany. E-mail: fuchsh@uni-muenster.de*

[b]*Park Systems Corp., KANC 4F, Iui-Dong, 906-10, Suwon 443-270, Republic of Korea*

[c]*Advanced Institute of Convergence Technology, Seoul National University, Suwon, 443-270, Republic of Korea*

[d]*School of Materials Science and Engineering, Gwangju Institute of Science and Technology (GIST), 1 Oryong-dong, Buk-gu, Gwangju 500-712, Republic of Korea. E-mail: keg@gist.ac.kr*

[e]*Department of Nanobio Materials and Electronics (WCU), Gwangju Institute of Science and Technology (GIST), 1 Oryong-dong, Buk-gu, Gwangju 500-712, Republic of Korea*

[f]*Department of Medical System Engineering, Gwangju Institute of Science and Technology (GIST), 1 Oryong-dong, Buk-gu, Gwangju 500-712, Republic of Korea*

[g]*Center for NanoTechnology (CeNTech), Heisenbergstr. 11, 48149 Münster, Germany*

† Electronic supplementary information (ESI) available. See DOI: 10.1039/c3nr02665e

or doxorubicin-loaded DNA-wrapped HNTs (HDD) on actin distribution of adenocarcinomic human alveolar basal epithelial A549 cells are demonstrated. Especially, detailed morphological changes of A549 cells after exposure to HDD for a varying period of incubation were monitored by scanning electron microscopy (SEM) and scanning ion conductance microscopy (SICM).

Results and discussion

DNA was applied in this study for wrapping HNTs to make them water-dispersible, as well as being a platform for loading doxorubicin. The pristine HNT (Fig. 1A) is insoluble in water, but it becomes highly water dispersible after interacting with DNA. It is reported that the interaction between DNA and HNTs induces a reorientation of the phosphate groups in DNA and an association of the phosphates in DNA with the outer surface of the nanotubes, which is composed of silica, was confirmed by FT-IR analysis.[4] Thus, π–π interaction is supposed to be a critical force to determine the interaction between DNA and the outer surface of HNTs. The TEM image (Fig. 1B) shows the morphology of DNA-wrapped HNTs (HD). Fig. 1C shows the light scattering intensity distribution as a function of HD size. There are two main regions of hydrodynamic sizes of HD near 128.2 nm and 735.3 nm related to the diameter of HD or shortened HD during preparation and length of HD, respectively. Although the DLS analysis method has been considered as a reasonable tool to estimate the length distribution of nanotubes, this method handles anisotropic rod-like particles as spherical particles within a hydrodynamic approximation.[9,23] For example, it is possible to estimate the diameter distribution of individual nanotubes using the DLS method as well-dispersed and individualized nanotubes can freely rotate at a certain concentration level.[23] To confirm the DLS results, therefore, the size (diameter and length) distribution of nanotubes obtained from TEM images is shown in Fig. S1.† It shows similar results as DLS, corroborating the above interpretation of the DLS data. Cytotoxicity of HD against A549 cells was evaluated by MTT assay. It shows a negligible cytotoxicity against A549 cells at a concentration of up to 250 $\mu g\ mL^{-1}$ for 1 day and around 90% of cell viability after exposure to HD at a concentration of higher than 500 $\mu g\ mL^{-1}$ as shown in Fig. 1D.

We selected doxorubicin (DOX) as a model drug to evaluate DNA-wrapped HNTs as a drug delivery carrier. DOX is one of the potential anticancer drugs which is a clinically approved chemotherapeutic agent. Its functional mechanism is supposed to be based on binding to duplex DNA (dsDNA) *via* sequence specific intercalation inducing cellular apoptosis.[24] There are two suggested mechanisms to load DOX to DNA-wrapped HNTs. First, DOX intercalates with DNA and secondly, DOX, which is a cationic drug, is adsorbed onto the surface of the tubules by electrostatic attraction. Intercalating DOX into DNA was reported and it induces quenching of DOX fluorescence.[25] In addition, the change in surface charges after loading DOX supports interactions between DOX and HD. The zeta-potential of HD is -62.9 ± 0.5 mV, which is highly negative, and that of HDD is -37.4 ± 0.3 mV because of DOX loading. The amount of DOX intercalated with DNA and adsorbed onto HNT or HD surfaces was calculated by correlating with a standard curve of the fluorescence intensity of DOX. Three batches of HDD were analyzed. The average amount of DOX in HDD is 5.2 $\mu g\ mg^{-1}$. Fig. 2A shows the morphology of doxorubicin-loaded DNA-wrapped HNTs (HDD). The HDD is also well-dispersed in water. Fig. 2B shows two main light scattering intensity distributions around 56.6 nm and 751.2 nm indicating the diameters of HDD or shortened HDD during preparation and length of HDD, respectively.

We compared the cytotoxicity of pristine DOX and HDD against adenocarcinomic human alveolar basal epithelial A549 cells. As shown in Fig. 3, the A549 cells are very sensitive to pristine DOX; IC_{50} values are in the low nano-molar range after 2 and 3 day treatments. Compared to free DOX, there is no

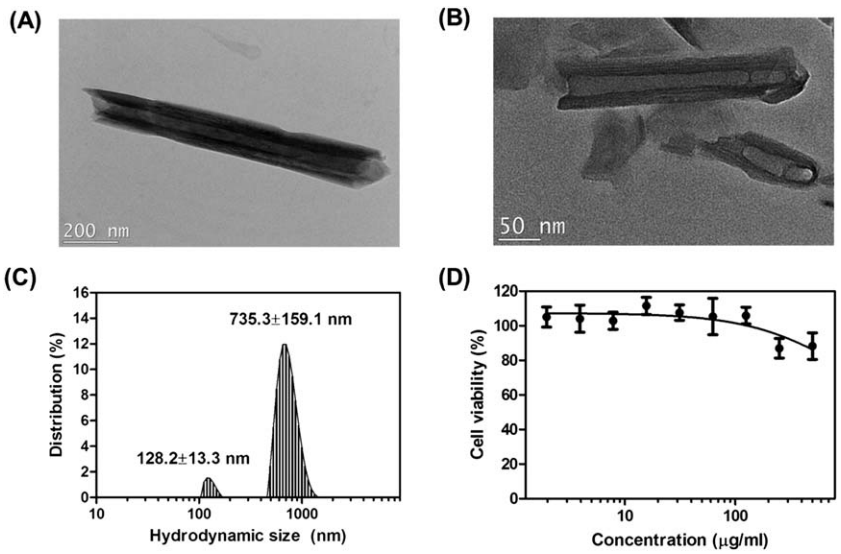

Fig. 1 TEM images of (A) pristine HNTs and (B) DNA-wrapped HNTs (HD), (C) size distribution of HD obtained by dynamic light scattering, and (D) A594 cell viability after exposure to HD for 1 day (control: cell viability of A549 cells without treatment is 100%).

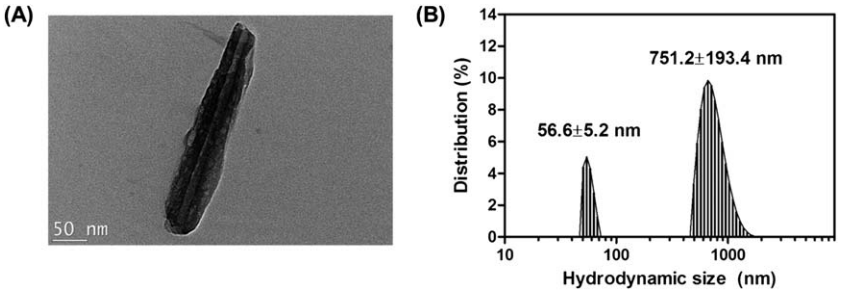

Fig. 2 (A) TEM image of doxorubicin-loaded, DNA-wrapped halloysite nanotubes (HDD) and (B) hydrodynamic size distribution of HDD measured by a dynamic light scattering method.

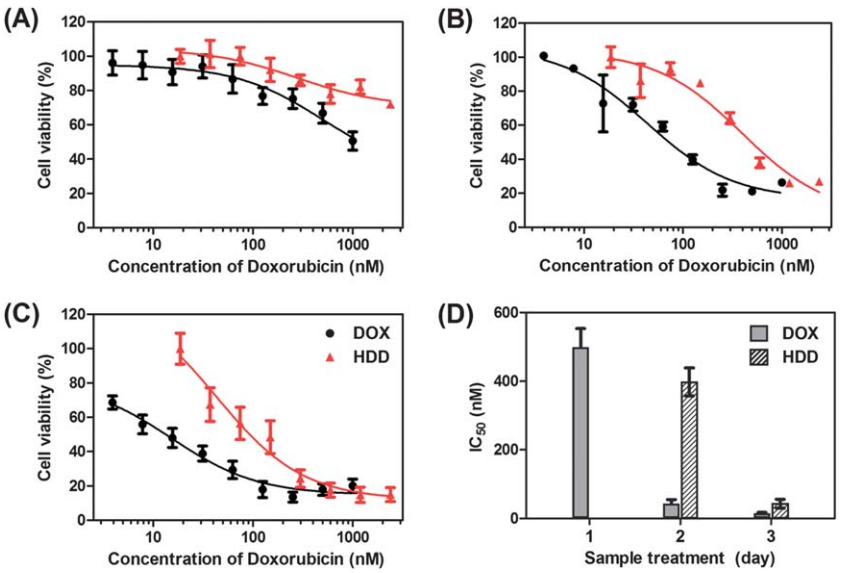

Fig. 3 A549 cell viability after treatment of DOX or HDD for (A) 1 day, (B) 2 days, and (C) 3 days ($n = 4$). Cell viability of control (untreated A549 cells): 100%. (D) Comparison of IC_{50} (nM) values (calculation of the IC_{50} value of A549 cells after treatment of HDD for 1 day is not available).

considerable cancer cell-inhibition effect of HDD within 1 day; A549 cell viability at a net concentration of 1.25 μM DOX in HDD is around 80%, while the IC_{50} value of free DOX is 499.0 ± 54.4 nM. The effect of HDD is enhanced when A549 cells were exposed longer than 2 days. Nevertheless, free DOX is still more cytotoxic. After 3 days of treatment, the IC_{50} value of DOX is 15.3 ± 2.5 nM and HDD is 43.1 ± 13.3 nM. These results demonstrate slow DOX release from HDD.

The confocal laser scanning micrographs shown in Fig. 4 clearly support a different release rate between DOX and HDD after being taken up by A549 cells. Free DOX readily diffused into the cellular membrane of A549 cells within 2 hours and exclusively stained nuclei as well as cytoplasm, while weak red fluorescence of localized HDD or released DOX from HDD in A549 cells was observed under the same cellular incubation conditions. After 6 hours of treatment, the same type of distribution of red fluorescence in A549 cells was observed. However, after 24 hours of treatment of HDD, strong red fluorescence was observed in nuclei as well as cytoplasm suggesting increased concentration of HDD localized in cellular compartments as well as accumulation of released DOX from HDD. It is expected that a reduced DOX release during the initial phase would contribute to minimize toxic effects of DOX on normal tissues after administration and DOX-loaded DNA wrapped HNTs can be ideal sustained drug delivery systems.

DOX release from HDD was investigated in a physiological pH environment (pH: 7.4) over 2 weeks. To be a promising drug delivery system, a constant release rate with time is crucial.[15,26] The initial concentration of injected or ingested conventional drugs is high in the blood stream, and falls off exponentially in blood concentration with time. A high level of drugs after initial administration leads to toxicity and diminished drug concentration requires additional doses. Hence, a retarded release system will be ideal because in this case the blood level of drugs remains constant throughout a prolonged delivery period. In most cases, the release profiles display two main processes. First, an initial burst of pharmaceutical molecules is observed indicating loosely bound molecules on the surface of cargo molecules, which are released in a short period of time. Then, more constant release rates are monitored depending on release of pharmaceutical molecules from cargo molecules.[15,26] Fig. S2† shows the DOX release profile over 2 weeks. It is reported that free

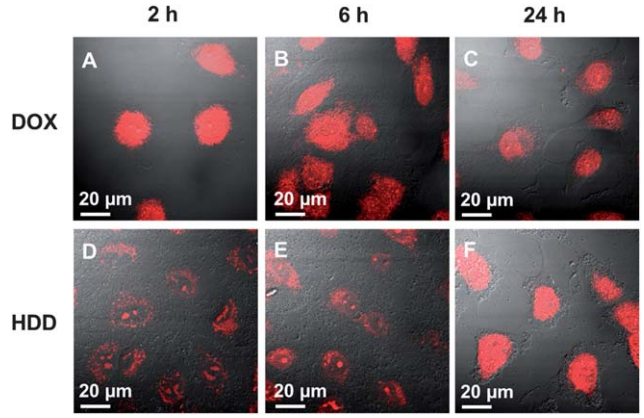

Fig. 4 Confocal microscopic images of DOX and HDD localization in A549 cells (*z*-section: 2.5 μm; 1 μM of DOX and 200 μg mL^{-1} of HDD were treated).

DOX rapidly released from the dialysis bag; more than 80% of the free DOX was released in 5 hours. In our study, there is no significant initial burst of DOX from HDD in the initial phase and a constant release of DOX over 2 weeks is monitored.

The plasma membrane is one of the major components of cell architecture. It defines the exterior of the cells and plays a role in the first barrier to control the transport of molecules in an extracellular medium into the cell by various pathways.[27] Endocytosis is the general pathway for various xenobiotic materials classified into phagocytosis and pinocytosis. Phagocytosis is restricted to specialized cells such as macrophages, monocytes, and neutrophils, and represents the internalization process of particulate substances larger than a few tenths of a micrometer in diameter. Pinocytosis includes macropinocytosis (for particles >1 μm), clathrin-mediated endocytosis, caveolin-mediated endocytosis, and clathrin- and caveolin-independent endocytosis.[27] When extracellular materials such as nanoparticles or microparticles are taken up by endocytosis or phagocytosis, the cellular membrane is invaginated and, simultaneously, it induces the reorganization of the cytoskeleton, which is a dense network of three classes of protein filaments, namely, intermediate filaments, microtubules, and microfilaments, that mechanically support the cellular membrane and its internal compartments.[28] Several steps are shown in endocytic processes, membrane invagination, coated pit formation, coated pit sequestration, detachment of the newly formed vesicle, and movement of endocytic vesicles into the cytosol; each step may potentially involve the cytoskeleton.[29] Actin polymerization provides the force behind plasma membrane invagination or the pinching off of endocytic vesicles.[28]

To investigate the cellular uptake mechanism of HDD, in particular, cytoskeleton-dependent endocytosis, we compared the red fluorescence intensity of cells incubated with HDD to cells pre-treated with cytochalasin B (CytB), and then exposed to HDD. The CytB disrupts actin filaments, weakens existing actin filaments, and blocks actin polymerization.[30] By using confocal laser scanning microscopy (CLSM), we first confirmed the disruption of the cytoskeleton after treatment of 2.5 μg mL^{-1} CytB by visualizing F-actin using Alexa 488-conjugated phalloidin. In the control cells, strong peripheral F-actin staining along the cell edge is observed (Fig. 5A), while cells treated with CytB show actin dots rather than long stress fibers suggesting disruption of actin filaments (Fig. 5B). Also CytB significantly alters cellular morphology as shown by SEM (Fig. 5B). Control cells are well-spread in the substrate and their surface is smooth (Fig. 5A). When the cells are in the presence of CytB, most of the cells changed to round-shape and they are not to extent as the control cells (Fig. 5B). When A549 cells were exposed to HDD, the HDD or released DOX is mainly localized in cytoplasm and the perinuclear area and also in nuclei (Fig. 5C and D). However, the red fluorescent intensity from CytB pre-treated cells with treatment of HDD (Fig. 5D) is weaker than the cells co-cultured with HDD under regular conditions. Also, a relatively large amount of HDD is adsorbed on the cellular membrane (Fig. 5C); however, the surface of CytB-pretreated cells is smooth, even after exposure to HDD for 30 min, and only few particles are found as shown in Fig. 5D. Therefore, we conclude that HDD is taken up by A549 cells *via* cytoskeleton-dependent endocytosis.

As mentioned above, the cytoskeleton is an essential component of cells to maintain their shape, and further, modulate vital cellular functions such as force generation, motility, and division.[31] There are several factors, for example, exposure to foreign substances, oxidative stress, and radiation, which can induce damage to the cytoskeleton mammalian cells.[32] To investigate the effect of HDD on the actin structure, Alexa 488-conjugated phalloidin stained actin structures inside the cells were monitored over three different planes such as apical, median, and basal, using confocal laser scanning microscopy. In addition, morphological changes in HDD-treated A549 cells were observed using SEM and scanning ion conductance microscopy (SICM). In this study, detailed structural or functional changes of A549 cells after treatment with HDD for a certain time period were visualized by SEM and SICM. Both methods have their pros and cons. In the case of SEM analysis, there are several steps required to prepare samples such as fixation and dehydration and it may be possible to damage the samples during preparation. Also, the biological samples can be damaged from electrical charging, vacuum, and electron beam prior to inspection.[33] In contrast, SICM, which employs glass pipettes as ion sensitive scanning probes, is capable of simultaneously reporting various structural and functional parameters of biological specimens at nanometer-scale resolution in the physiological environment.[34,35]

Untreated cells are well spread with lamellipodia (Fig. 8A, SEM images) and dense and thick actin filaments are mainly localized in the basal plane (Fig. 6 and 7). To investigate the effect of drug carriers (HD) on A549 cells, the distribution of actin filaments in A549 cells co-cultured with HD at a concentration of 500 μg mL^{-1} was monitored. Fig. 6 shows the redistribution of actin filaments of an A549 cell in the presence of HD. With increasing co-incubation time with HD, high amounts of aggregated HD covered the A549 cell surface, but they are well-spread in the substrate as shown in Fig. S3.† The addition of HD to A549 cells results in a modification of the actin structure, even though there is no acute cell death generated by HD and no dramatic reduction of A549 cell proliferation was found after 1 day (Fig. 1D). Actin fibrils appear in the apical and middle focal plane with increasing

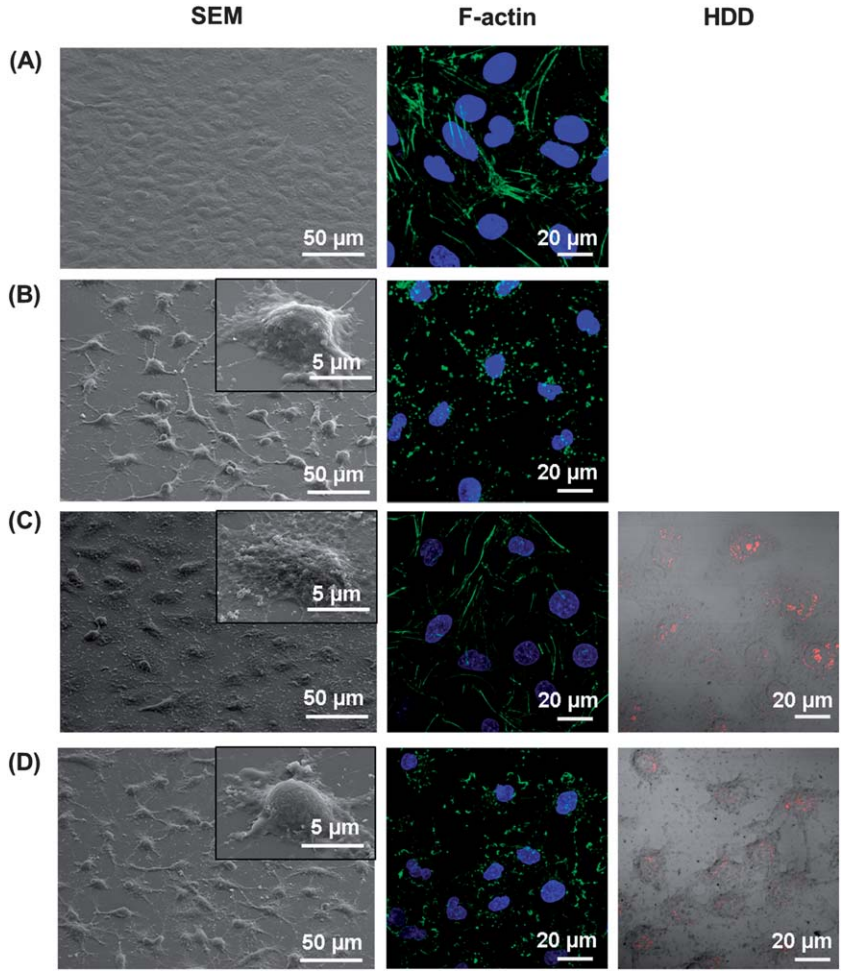

Fig. 5 SEM images and confocal laser scanning micrographs (*z*-stacks) visualizing F-actin stained by Alexa 488-conjugated phalliodin and localization of HDD (red fluorescence). (A) Untreated cells, (B) CytB (2.5 μg mL^{-1}) pre-treated cells, (C) HDD (200 μg mL^{-1})-treated A549 cells for 30 min under regular incubation conditions (37 °C, 10% CO2), and (D) A549 cells pre-treated with CytB for 30 min, and then exposed to HDD (200 μg mL^{-1}) for 30 min.

co-incubation time of HD and are also concentrated around the cell periphery. It is speculated that cellular uptake of HD induces actin redistribution rather than a toxic effect of HD on A549 cells. There are a few studies reporting the cytotoxicity of HNTs. For example, pristine HNTs or APTES-functionalized HNTs inhibited growth of MCF7 or HeLa cells in a concentration dependent manner; both exhibiting a cell viability less than 70% for HNT concentrations up to 75 μg mL^{-1}.[5] Another recent study reported that HNTs have no significant cytotoxic effect on A549 cells at a concentration up to 100 μg mL^{-1}, but a plate-type of nanoclay, cloisite Na^+, which has a similar chemical composition $[(Na,Ca)_{0.33}(Al,Mg)_2Si_4O_{10}(OH)_2]$ as HNTs, is highly cytotoxic due to its different specific surface area (HNTs: 65 m^2 g^{-1}, cloisite Na^+: 800 m^2 g^{-1}).[36] Both studies suggested that HNTs are biocompatible at a certain concentration range. However, there is no report concerning effects of HNTs on organization of actin filaments yet.

When cells were treated with HDD, delocalized actin filaments throughout the cells were found. After 2 hours of treatment, actin filaments became thinner and distribute throughout the cells. Additionally, the short spiky actin filaments in the peri-nuclear region are observed in the center focal-plane (Fig. 7). When we increased the sample treatment time to 12 hours, actin filaments are broken, aggregated, or appear disrupted and as an aspiration of dots suggesting either a depolymerization process or lack of actin filament synthesis. Also, adsorbed HDD or taken up HDD by the A549 cell surface after co-incubation is clearly observed in SEM images (Fig. 8). High resolution SICM images confirm the adsorption of HDD onto the A549 cell surface by evaluating topographical effects, including the formation of lamellipodia and filopodia. As the incubation time with HDD increased, A549 cell surfaces became rougher based on height profile comparisons. Indeed, the exposure of A549 cells to HDD induces structural defects in the cellular architecture, as indicated by a decrease in cellular volume in comparison to untreated cells. We expect that the presence of HDD induces major adverse effects on cell viability. The adsorption of HDD to cell surfaces suggests that membrane destabilization by this agent may lead to cell shrinkage as structural integrity is lost. In fact, various anticancer agents are purposely designed to target cell membranes and cytoskeleton, inducing cytotoxicity and alteration of cytoadherence.[37] DOX, which we used in this study, tethers to DNA and causes damage to the cell membrane by inducing peroxidation.[37] Collectively,

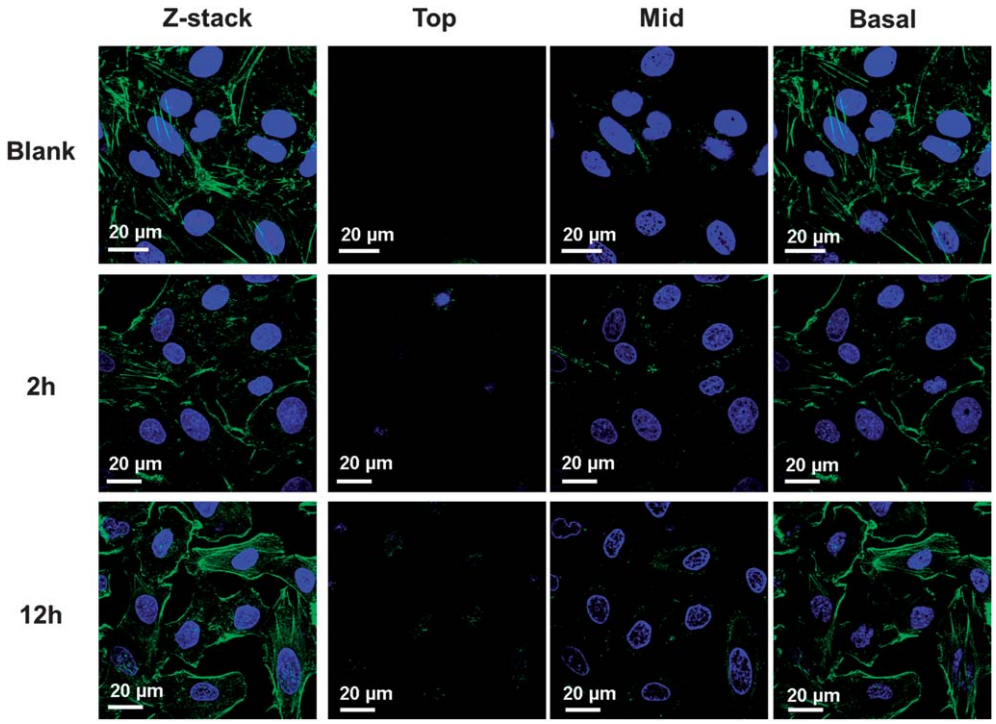

Fig. 6 Confocal microscopic images showing distribution of actin filaments in A549 cells by increasing exposure time of DNA-wrapped HNTs (blank: A549 cells without treatment, concentration of HD: 500 μg mL^{-1}).

the capability of SICM imaging to monitor cells under physiological conditions complements SEM imaging experiments and provides direct evidence that HDD acts by destabilizing cellular architecture, thereby offering a mechanistic explanation for the observed therapeutic effect of the HDD anticancer agent.

Conclusions

We have presented cellular interactions of water-dispersible HNT-based supramolecular complexes such as DNA-wrapped HNTs and DOX-loaded HD. Based on negligible cytotoxicity of HD and the slow release of DOX from HDD, HDD is considered as a promising sustained delivery system for DOX. The HD and HDD taken up by cells induce changes in cytoskeleton organization. Heterogeneous actin filaments throughout cells treated with HD or HDD were monitored. Specifically, disruption of actin filaments is shown in separated dot structures. Short spiky actin filaments were observed in A549 cells treated with HDD because of the release of DOX from HDD. In addition, detailed cellular morphological information obtained by SICM in a physiological environment showed adsorption of HDD on the cellular surface and cellular shrinkage in cell architecture with increasing exposure time to HDD.

Experimental section

Preparation of doxorubicin-loaded halloysite nanotubes (HDD)

The doxorubicin-loaded halloysite nanotubes were synthesized by a two-step high speed vibration milling process. The preparation method for the intermediate complex, DNA-wrapped HNTs (HD), was slightly modified compared to our previous work.[4] Halloysite was first sieved to remove granules using a 125 μm filter membrane. DNA (sodium salt of double-stranded DNA from herring testes, Sigma Aldrich, 25 mg) and halloysite nanotubes (HNTs, premium grade, New Zealand China Clays Ltd, 25 mg) were placed in a stainless steel capsule together with two stainless steel mixing balls. The samples were mixed vigorously at 20 Hz using a high-speed vibration mill (HSVM, MM 200, Retsch Co. Ltd.) at ambient temperature for 30 min. The stock solution of doxorubicin hydrochloride (DOX, AK Scientifics Inc., 2 mg mL^{-1}) was prepared in double deionized water. 1 mL of DOX was added to a stainless steel capsule containing intermediate complexes of DNA and HNTs and mixed at 20 Hz using a high-speed vibration mill system for another 30 min. The final product was dissolved into water (30 mL) and centrifuged (Vision centrifuge, VS-5000N) at 2500 rpm at 30 min. Then, the supernatant was collected and dialyzed for 2 days using a regenerated-cellulose dialysis tubing (SnakeSkin Dialysis Tubing, 3.5K MWCO, Thermo Scientific) in the dark and freeze-dried using a freeze drying system from Samwon Engineering (Model: SFDSM12).

Characterizations of complexes

The morphology of the complex such as HD and HDD was monitored by scanning electron microscopy (SEM, Hitachi S-4700) and transmission electron microscopy (TEM, JEOL TEM-2100, accelerating voltage = 200 kV). The particle size and surface charge were measured by dynamic light scattering (DLS)

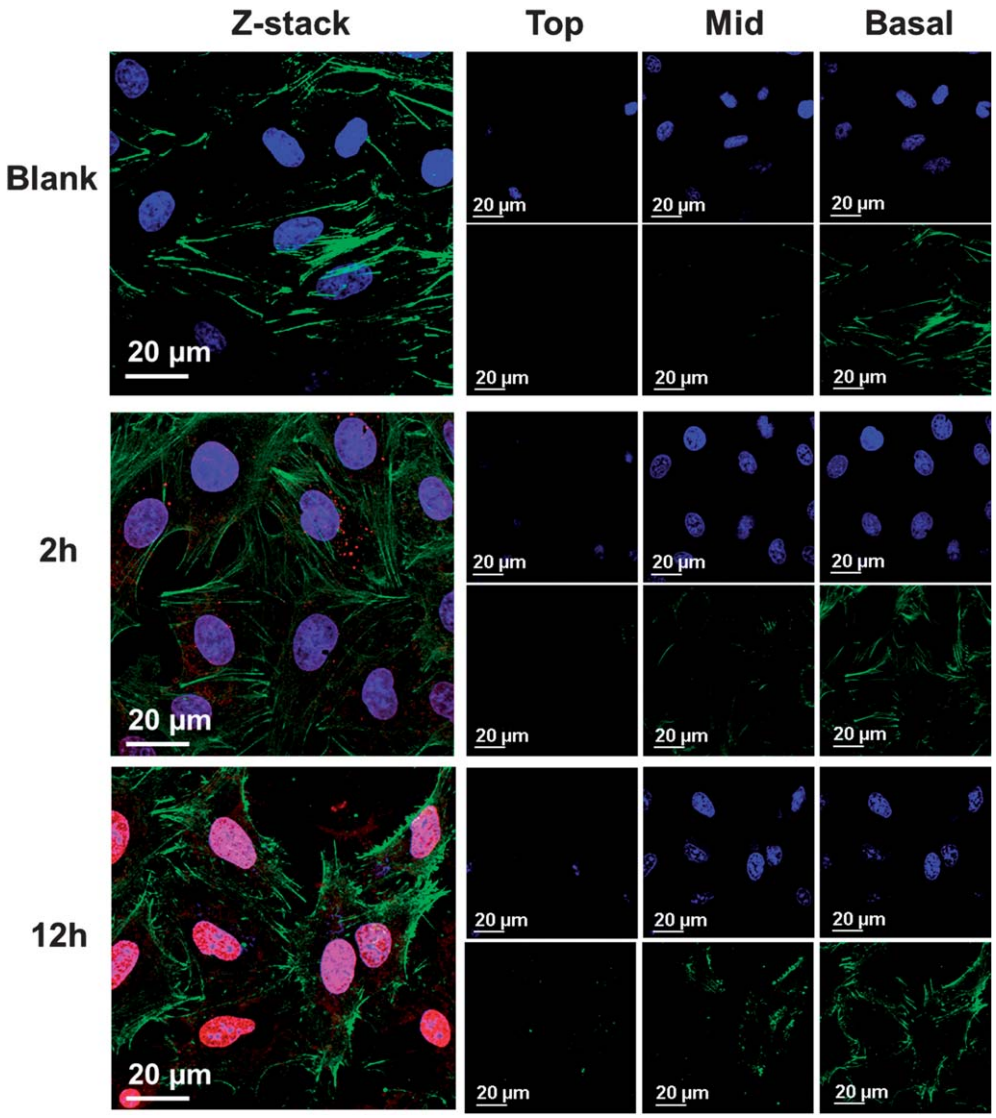

Fig. 7 Confocal images of A549 cells showing F-actin distribution in control cells and the cells with treatment of HDD (500 μg mL^{-1}) for 2 hours and 12 hours. (Blue fluorescence: nuclei stained by Hoechst 33258, green fluorescence: F-actins stained by Alexa 488-conjugated phalliodin, and red fluorescence: HDD or released DOX.)

and the zeta-potential, respectively, on an ELS-Z system (Otsuka Electronics Co., Ltd.).

Cell culture

Adenocarcinomic human alveolar basal epithelial A549 cells were purchased from the Korean Cell Line Bank (KCLB) and were cultured in Dulbecco's Modified Eagle's Medium (Sigma Aldrich) supplemented with 10% FBS (Sigma Aldrich) and 1% Antibiotic–Antimycotic (Gibco) in the presence of 10% CO_2 and 37 °C.

MTT assay

The cytotoxicity of the DOX and formulated complex (HDD) was measured using the MTT colorimetric assay with A549 cells. 10 mM DOX stock solution was prepared in DMSO (Junsei) and diluted in cell culture media. HDD was dissolved in PBS (pH 7.4) at a concentration of 10 mg mL^{-1}. The A549 cells were seeded in a 96-well plate at a density of 1×10^4 cells per well and incubated overnight. After treating the samples for a certain time period (1, 2, and 3 days, respectively), the cells were thoroughly rinsed using pre-warmed PBS. Then MTT solution (5 mg mL^{-1} in PBS, Thiazoyl Blue Tetrazolium Bromide, Sigma-Aldrich) was added. The purple-colored MTT formazan formed in living cells was solubilized in DMSO. The absorbance was then measured at 570 nm using a microplate reader (SpectraMax M2, Molecular Devices).

Cellular uptake of HDD

Cellular uptake of DOX and HDD was monitored by confocal laser scanning microscopy (CLSM, Olympus FluoView FV1000). 2×10^5 A549 cells were seeded on a 12-well cell culture plate containing sterilized glass coverslips (diameter: 15 mm) for 1 day. The cells were incubated for 30 min with cell culture media or 2.5 μg mL^{-1} of cytochalasin B (CytB) to disrupt the cytoskeleton. Then, 200 μg mL^{-1} of HDD was added and incubated for 30 min. After treatment

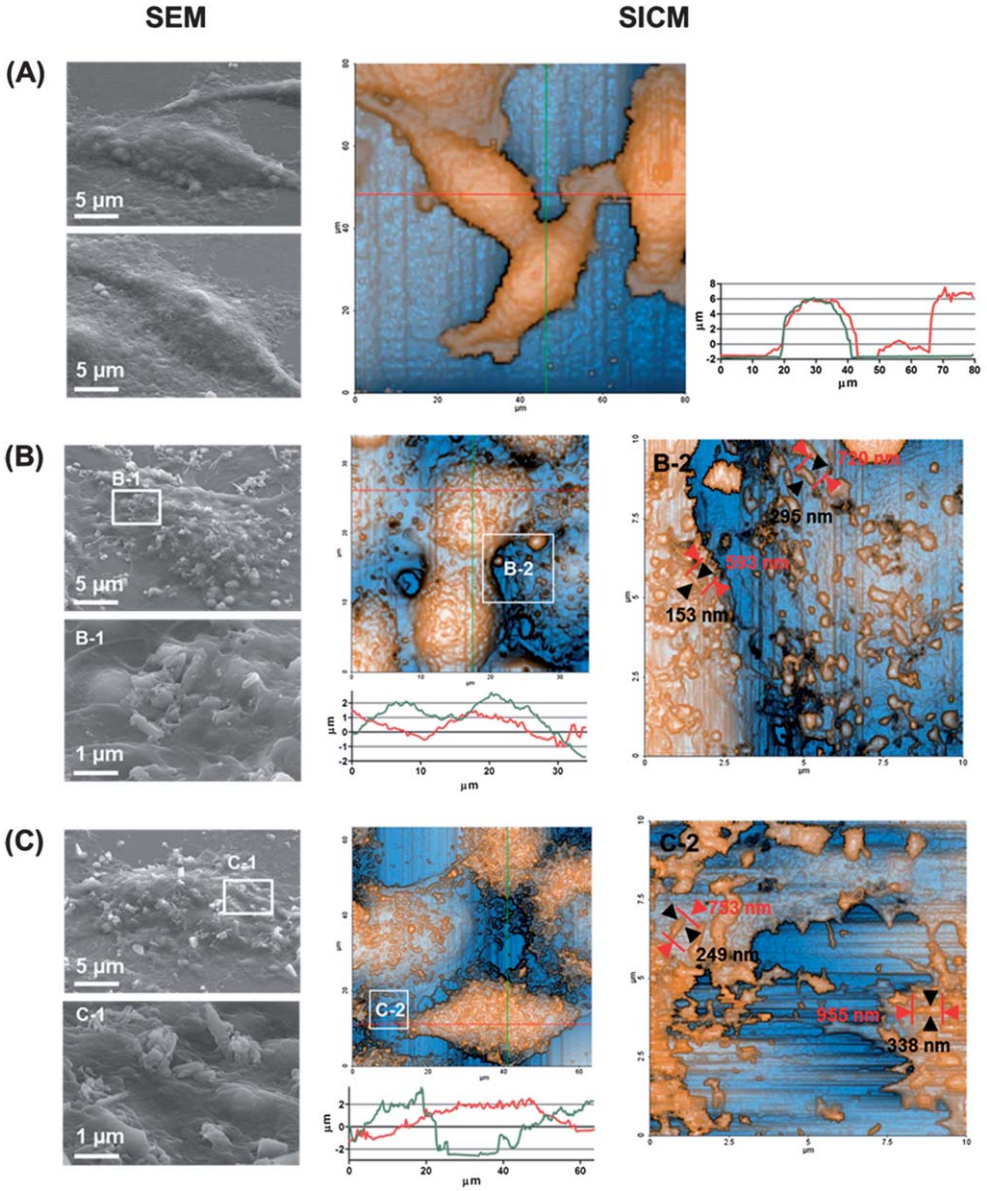

Fig. 8 SEM (left) and SICM (right) images (enhanced color mode) with height profiles (red and green lines) of (A) untreated A549 cells, after exposure to HDD (500 μg mL^{-1}) for (B) 2 hours and (C) 12 hours. Normal mode of SICM images with a *z*-axis scale attached in the ESI, Fig. S4.†

of HDD, cells were rinsed with pre-warmed PBS and were fixed using 4% paraformaldehyde (32% paraformaldehyde aqueous solution was purchased from Electron Microscopy Sciences and diluted) for 10 min at room temperature. The fixed cells were permeabilized with 2% Triton X-100 (Sigma Aldrich) solution for 10 min at room temperature and blocked using 2% bovine serum albumin (Sigma Aldrich) for 10 min. Then the cells were stained using Alexa Fluor® 488 Phalloidin (1 : 250, Invitrogen) for 1 hour, and the nuclei were stained using Hoechst 33258 (Sigma Aldrich) for 10 min at room temperature. The localized HDD and cytoskeleton of A549 cells were visualized by CLSM.

Morphological changes of A549 cells

1×10^5 A549 cells were seeded on a 12-well cell culture plate containing sterilized glass coverslips (diameter: 15 mm) for scanning electron microscope (SEM) analysis and a surface-treated coverglass-bottom dish (SPL Life Science) for scanning ion conductance microscope (SICM) analysis. Cells were cultured under regular incubation conditions (37 °C, 10% CO_2). After treatment of HDD (500 μg mL^{-1}) for a certain time period, cells were rinsed using pre-warmed PBS and fixed with 4% paraformaldehyde.

For SEM analysis, the paraformaldehyde-fixed cells were fixed again in 2% osmium tetroxide (Electron Microscopy Sciences), and then they were dehydrated through a series of ethanol concentrations (30%, 50%, 70%, 80%, 90%, 95%, and 100%). Once dry, the cells were sputter coated with platinum and their surface structure was observed using a Hitachi S-4700 SEM (accelerating voltage: 10 kV).

For SICM analysis, an XE-Bio instrument (Park Systems) was employed. First, 1 × PBS buffer was added to a Petri dish containing fixed cells in 4% paraformaldehyde. After inserting the

bath electrode (the Ag–AgCl disk electrode) into the Petri dish, a current of 100 mV was applied. A pipette filled with 1 × PBS was then immersed into the Petri dish by control of the *z*-axis motor. After immersion, ion current flow (I) through the pipette could be measured by the current amplifier (10^9 gain). As the pipette approached the cell surface, the resistance increases and in turn results in a decrease of ion current flow. The point at which this occurs can be selected as the set point value (normally 1–2% of I_{max}). Taken together with positional feedback from the motion of the pipette, monitoring the change in the ion current flow can provide a three-dimensional spatial map of the cell morphology. The SICM pipettes were fabricated using a borosilicate capillary (Sutter Instruments, USA) with an outer diameter of 1.00 mm and an inner diameter of 0.58 mm, with a CO_2-laser-based micropipette puller (P-2000, Sutter Instruments, Novato, CA). The diameter of the nano-pipette tip is in the range of 60–100 nm. The obtained images were analyzed by XEI software.

Statistical analysis

The data are expressed as mean ± standard deviation. IC_{50} values were calculated by GraphPad Prism 5.0 software using sigmoidal dose–response analysis.

Acknowledgements

This work was supported in part by the World-Class University (WCU) program through a grant provided by the Ministry of Education, Science and Technology (MEST) of Korea (Project no. R31-10026).

References

1 M. Du, B. Guo and D. Jia, *Polym. Int.*, 2010, **59**, 574.
2 Y. M. Lvov, D. G. Shchukin, H. Möhwald and R. R. Price, *ACS Nano*, 2008, **2**, 814.
3 C. Breen, N. D'Mello and J. Yarwood, *J. Mater. Chem.*, 2002, **12**, 273.
4 M. H. Shamsi and K. E. Geckeler, *Nanotechnology*, 2008, **19**, 075604.
5 V. Vergaro, E. Abdullayev, Y. M. Lvov, A. Zeitoun, R. Cingolani, R. Rinaldi and S. Leporatti, *Biomacromolecules*, 2010, **11**, 820.
6 N. G. Veerabadran, D. Mongayt, V. Torchilin, R. R. Price and Y. M. Lvov, *Macromol. Rapid Commun.*, 2009, **30**, 99.
7 D. Rawtani and Y. K. Agrawal, *Rev. Adv. Mater. Sci.*, 2012, **30**, 282.
8 K. E. Geckeler and H. Nishide, *Advanced Nanomaterials*, Wiley-VCH, Weinheim, Germany, 2009.
9 Y. Lee and K. E. Geckeler, *Macromol. Rapid Commun.*, 2011, **32**, 1518.
10 Y. Lee and K. E. Geckeler, *Macromol. Biosci.*, 2012, **12**, 1060.
11 D. S. Kommireddy, I. Ichinose, Y. M. Lvov and D. K. Mills, *J. Biomed. Nanotechnol.*, 2005, **1**, 286.
12 W. Y. Zhou, B. Guo, M. Liu, R. Liao, A. B. M. Rabie and D. Jia, *J. Biomed. Mater. Res., Part A*, 2010, **93**, 1574.
13 M. Liu, Y. Zhang, C. Wu, S. Xiong and C. Zhou, *Int. J. Biol. Macromol.*, 2012, **51**, 566.
14 Y. J. Suh, D. S. Kil, K. S. Chung, E. Abdullayev, Y. M. Lvov and D. Mongayt, *J. Nanosci. Nanotechnol.*, 2011, **11**, 661.
15 V. Vergaro, Y. M. Lvov and S. Leporatti, *Macromol. Biosci.*, 2012, 1265.
16 W. Wei, E. Abdullayev, A. Hollister, D. Mills and Y. M. Lvov, *Macromol. Mater. Eng.*, 2012, **297**, 645.
17 H. M. Kelly, P. B. Deasy, E. Ziaka and N. Claffey, *Int. J. Pharm.*, 2004, **274**, 167.
18 A. Ghebaur, S. A. Garea and H. Iovu, *Int. J. Pharm.*, 2012, **436**, 568.
19 R. Qi, R. Guo, M. Shen, X. Cao, L. Zhang, J. Xu, J. Yu and X. Shi, *J. Mater. Chem.*, 2010, **20**, 10622.
20 Y.-F. Shi, Z. Tian, Y. Zhang, H.-B. Shen and N.-Q. Jia, *Nanoscale Res. Lett.*, 2011, **6**, 1.
21 F. Arcamone, *Cancer Res.*, 1985, **45**, 5995.
22 O. Tacar, P. Sriamornsak and C. R. Dass, *J. Pharm. Pharmacol.*, 2013, **65**, 157.
23 J. Y. Lee, J. S. Kim, K. Hyeok An, K. Lee, D. Y. Kim, D. J. Bae and Y. H. Lee, *J. Nanosci. Nanotechnol.*, 2005, **5**, 1045.
24 N.-T. Chen, C.-Y. Wu, C.-Y. Chung, Y. Hwu, S.-H. Cheng, C.-Y. Mou and L.-W. Lo, *PLoS One*, 2012, **7**, e44947.
25 G. J. Schuurhuis, H. J. Broxterman, J. H. de Lange, H. M. Pinedo, T. H. van Heijningen, C. M. Kuiper, G. L. Scheffer, R. J. Scheper, C. K. van Kalken and J. P. Baak, *Br. J. Cancer*, 1991, **64**, 857.
26 S. Freiberg and X. X. Zhu, *Int. J. Pharm.*, 2004, **282**, 1.
27 B. Alberts, A. Johnson, J. Lewis, M. Raff, K. Roberts and P. Walter, *Molecular Biology of The Cell*, Garland Science, Taylor & Francis Group, New York, 5 edn, 2008.
28 R. L. Jeng and M. D. Welch, *Curr. Biol.*, 2001, **11**, R691.
29 B. Qualmann, M. M. Kessels and R. B. Kelly, *J. Cell Biol.*, 2000, **150**, 111.
30 R. E. Serda, J. Gu, R. C. Bhavane, X. Liu, C. Chiappini, P. Decuzzi and M. Ferrari, *Biomaterials*, 2009, **30**, 2440.
31 B. D. Holt, P. A. Short, A. D. Rape, Y.-l. Wang, M. F. Islam and K. N. Dahl, *ACS Nano*, 2010, **4**, 4872.
32 J. Kanungo and M. Paule, *Mol. Cell. Biochem.*, 2011, **353**, 283.
33 Y. Zhang, X. Hu, J. Sun, Y. Shen, J. Hu, X. Xu and Z. Shao, *Microsc. Res. Tech.*, 2011, **74**, 614.
34 M. Miragoli, A. Moshkov, P. Novak, A. Shevchuk, V. O. Nikolaev, I. El-Hamamsy, C. M. F. Potter, P. Wright, S. H. S. A. Kadir, A. R. Lyon, J. A. Mitchell, A. H. Chester, D. Klenerman, M. J. Lab, Y. E. Korchev, S. E. Harding and J. Gorelik, *J. R. Soc., Interface*, 2011, **8**, 913.
35 T. Ushiki, M. Nakajima, M. Choi, S.-J. Cho and F. Iwata, *Micron*, 2012, **43**, 1390.
36 N. Verma, E. Moore, W. Blau, Y. Volkov and P. Ramesh Babu, *J. Nanopart. Res.*, 2012, **14**, 1.
37 S. Suresh, *Acta Biomater.*, 2007, **3**, 413.